

Simplified laser-speckle-imaging analysis method and its application to retinal blood flow imaging

Haiying Cheng¹ and Timothy Q. Duong²

Yerkes Imaging Center, Department of Neurology, Emory University, Atlanta, Georgia 30329, USA

¹hcheng4@emory.edu

²tduong@emory.edu

Received March 14, 2007; revised June 4, 2007; accepted June 5, 2007;
posted June 11, 2007 (Doc. ID 81061); published July 23, 2007

Laser speckle imaging (LSI) is widely used to study blood flow at high spatiotemporal resolution. Several papers recently pointed out that the commonly used LSI equation involves an approximation that could result in incorrect data analysis. We investigated the impact of such an approximation and introduced a simplified analysis method to improve computation time. Flow phantom studies were performed for validation. Moreover, we demonstrated a novel LSI application by imaging blood flow of rat retinas under normal and physiologic-challenge conditions. Because blood-flow abnormality is implicated in many retinal diseases, LSI could provide valuable physiologic, and potentially diagnostic, information. © 2007 Optical Society of America

OCIS codes: 170.6480, 170.3880, 170.4470.

Laser speckle imaging (LSI) [1] can be used to image instantaneous velocity distribution *in vivo* at very high spatiotemporal resolution, an improvement over the single point techniques, such as laser Doppler flowmetry [2]. Laser speckle is an optical interference effect. The speckle pattern fluctuates if the illuminated area contains moving particles such as moving red blood cells. By integrating the intensity fluctuations of the speckle pattern over a finite time, information about the motion of the scattering particles could be derived. LSI has recently been applied to image changes in cerebral blood flow associated with focal brain ischemia and cortical spreading depression in rats [3]. LSI has since proven to be a cost-effective technique for measuring dynamic blood flow changes at very high spatiotemporal resolution [4,5]. However, several papers [6–8] recently pointed out that the commonly used LSI equation involves an approximation that could result in incorrect data analysis.

In this study, we investigated the contribution of such approximation and its impact on LSI data analysis and proposed a simplified LSI analysis method to speed up computation time. For validation, we performed flow phantoms experiments at different physiological flow rates and different camera exposure times. Moreover, we demonstrated a novel *in vivo* application by imaging blood flow of the rat retinas in which the animals breathed air or oxygen. The latter was used to modulate blood flow for testing sensitivity. LSI blood-flow index maps and physiologically induced percent-change maps were analyzed.

Speckle contrast (K) is defined in terms of the standard deviation (σ_s) and the mean local spatial speckle intensity fluctuations ($\langle I \rangle$). Per Fercher and Briers' formalism, the relation between speckle contrast and spatial variance of the time-averaged speckle pattern is [1]

$$K = \sigma_s / \langle I \rangle = \sqrt{\int_0^T |g(\tau)|^2 d\tau / T} \quad (\text{Method I}), \quad (1a)$$

where $g(\tau)$ is the normalized autocorrelation function, τ is the lag time, and T is the CCD camera exposure time. Assuming a Lorentzian spectrum, $g(\tau) = \exp(-|\tau|/\tau_c)$, where τ_c is the correlation time, Eq. (1a) can be rewritten as

$$K = \sigma_s / \langle I \rangle = [(\tau_c/2T)\{1 - \exp(-2T/\tau_c)\}]^{1/2} \quad (\text{Method I}), \quad (1b)$$

where T/τ_c is proportional to the mean velocity [9] V and is the blood-flow index.

However, in Goodman's original master LSI equation [10], the speckle contrast is related to the spatial variance in the time-averaged speckle pattern by

$$K = \sigma_s / \langle I \rangle = \sqrt{\frac{1}{T} \int_{-\infty}^{\infty} \Lambda\left(\frac{\tau}{T}\right) |g(\tau)|^2 d\tau} \quad (\text{Method II}), \quad (2a)$$

where

$$\Lambda\left(\frac{\tau}{T}\right) = \begin{cases} 1 - \frac{|\tau|}{T} & \frac{|\tau|}{T} \leq 1 \\ 0 & \text{otherwise} \end{cases}$$

or

$$K = \sigma_s / \langle I \rangle = \sqrt{\int_0^T 2\left(1 - \frac{\tau}{T}\right) |g(\tau)|^2 d\tau / T} \quad (\text{Method II}). \quad (2b)$$

Note that the factor $(1 - \tau/T)$ was approximated to unity in Eq. (1a) to simplify the integration. Assum-

ing a Lorentzian spectrum, Eq. (2b) can be rewritten as [11]

$$K = \sigma_s / \langle I \rangle = [\tau_c / T + 1/2(\tau_c / T)^2 \times \{\exp(-2T/\tau_c) - 1\}]^{1/2} \quad (\text{Method II}). \quad (2c)$$

It is unknown how such an approximation impacts LSI data analysis [6–8].

A typical laser diode in LSI experiments [3–5,7,12] has a wavelength spread $\Delta\lambda > 0.1$ nm and a mean wavelength $\bar{\lambda} \sim 780$ nm, which yields a coherence time $\tau_c = \bar{\lambda}^2 / (c\Delta\lambda)$ of $\sim 10^{-12}$ s. For $T = 1\text{--}40$ ms, T/τ_c is $> 10^9$. Substituting x for T/τ_c and y for $1/K^2$, Eq. (1b) becomes

$$y = \frac{2x}{1 - \exp(-2x)}, \quad \text{and}$$

$$\text{when } x \rightarrow \infty, y = 2x \text{ or } 1/K^2 = 2T/\tau_c \quad (\text{Method I}) \quad (3)$$

and Eq. (2c) becomes

$$y = \frac{x}{1 - [1 - \exp(-2x)]/2x}, \quad \text{and}$$

$$\text{when } x \rightarrow \infty, y = x \text{ or } 1/K^2 = T/\tau \quad (\text{Method II}). \quad (4)$$

Because $1/K^2$ is measured, the blood-flow index T/τ_c calculated from the asymptotic approximation ($x \rightarrow \infty$) of Method I is half of that of Method II. However, the percent changes between a stimulation and basal condition calculated using Eqs. (3) and (4) are identical. This analysis shows that the approximation of $(1 - \tau/T)$ to unity is valid for calculating blood-flow change when T/τ_c is large. Figure 1 graphically demonstrates this point and the asymptotic approxi-

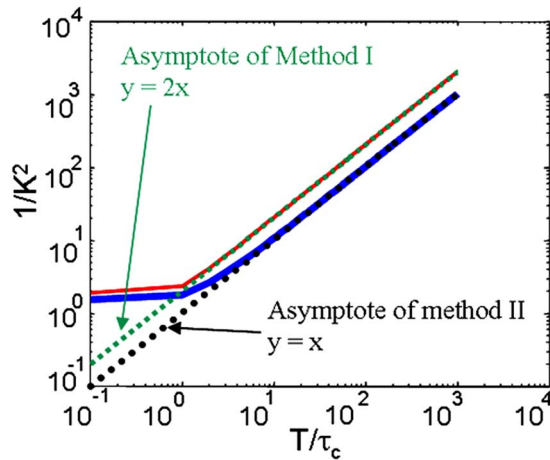


Fig. 1. (Color online) $1/K^2$ versus T/τ_c . $1/K^2$ versus flow velocity index of Method I [Eq. (1b)] is depicted by the thinner solid curve and that of Method II [Eq. (2c)] by the thicker solid curve. Their corresponding asymptotes [Eqs. (3) and (4)] are shown as dotted lines. Note that it is not apparent that the slope of Eq. (3) is twice that of Eq. (4) because log scales are plotted.

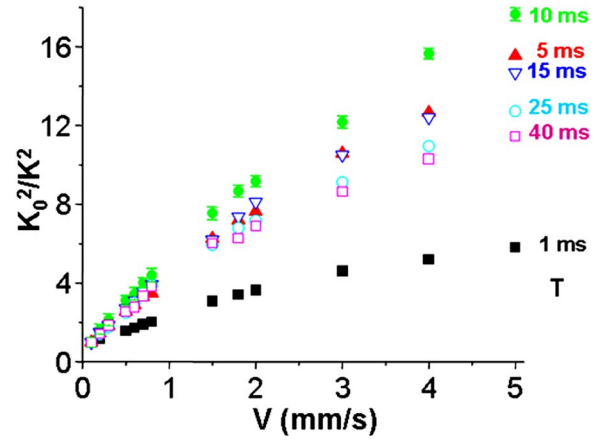


Fig. 2. (Color online) Normalized value of K_0^2/K^2 versus mean velocity V at different camera exposure times T obtained from flow phantoms. Normalization was performed with respect to the speckle contrast at the lowest velocity index (K_0) for each exposure time such that all data with different T can be plotted on the same scale. Standard-deviation error bars are shown for the LSI data obtained with $T = 10$ ms; error bars for other exposure times of similar magnitudes are omitted for clarity.

mation is valid for $T/\tau_c > 100$. This approximation should also hold for non-Lorentzian (such as Gaussian) spectra [11].

The Newtonian iterative method is often utilized to calculate the blood-flow index T/τ_c via Eq. (1b) or (2c). This calculation is computationally expensive for large time-series data sets. In contrast, the asymptotic approximation shows that the blood-flow index T/τ_c is linearly related to $1/K^2$ [Eqs. (3) and (4)]. We therefore propose that this asymptotic approximation could be used to simplify the LSI analysis method when calculating blood-flow change.

To validate this asymptotic approximation and the simplified LSI analysis method, we performed flow phantom experiments at different physiologic flow rates and different exposure times. The flow phantom consisted of 1% intralipid solution flowing in the polyethylene tubing (PE-50, 0.58 mm inner diameter) with mean velocities of 0 to 5 mm/s, generated via a digital syringe pump. LSI was performed on a vibration-isolation table using a 780 nm laser diode with $\Delta\lambda \sim 1$ nm and a modified commercial imager (Imager 3001, Optical Imaging, Mountainside, N.J.) at 25 Hz and $7 \mu\text{m}$ resolution. Figure 2 shows the normalized K_0^2/K^2 versus known flow velocity V of the flow phantoms obtained at different exposure times T . K_0^2/K^2 versus V were linearly correlated ($R^2 = 0.97$ to 0.99) for all exposure times and velocity ranges studied, validating the asymptotic approximation and the simplified analysis method. The slope was largest for $T = 10$ ms, indicating the optimal exposure time.

To demonstrate a novel application, we applied this approach to image blood flow in the retinas of three rats in which the animals breathed air followed by oxygen. Rats were anesthetized under $\sim 1\%$ isoflurane, mechanically ventilated, and paralyzed with pancuronium bromide (3 mg/kg first dose followed by

1 mg/kg/h, intraperitoneal administration). End-tidal carbon dioxide, heart rate, arterial oxygen saturation, and rectal temperature were monitored and maintained within normal physiologic ranges. LSI experiments were performed on a vibration-isolation table. Time-series LSI data using $T=10$ ms were collected over 3 min of air breathing and 3 min oxygen breathing. Two to four trials were acquired for each animal. Figure 3 shows the steady-state blood flow index maps of an animal breathing air and oxygen. The blood-flow index obtained by Newtonian iterative analysis of Method I [Eq. (1b), Fig. 3(A)] was half of that by Newtonian iterative analysis of Method II [Eq. (2c), Fig. 3(B)], as indicated by differences in scale bars. Both analysis Methods I and II, however, yielded identical percent-change maps between oxygen and air breathing. Importantly, the blood-flow index maps and the percent-change maps calculated using the simplified analysis of Method II [Eq. (4), Fig. 3(C)] were indistinguishable from Newtonian iterative analysis of Method II [Fig. 3(B)], confirming the validity of the asymptotic approximation and the simplified analysis method.

Moreover, blood flow in the retina was found to markedly decrease under oxygen breathing relative to air. This is because oxygen potently vasoconstricts retinal vessels, consistent with previous reports us-

ing laser Doppler flowmetry [13,14]. These results demonstrated the feasibility of imaging physiologically evoked blood flow changes in the retina at very high spatiotemporal resolution in a totally noninvasive manner.

It is interesting to note that T/τ_c ranges from 100 to 400 in typical *in vivo* LSI experiments [3–5,7,12] including our study. This value is much smaller than the theoretical prediction because speckle contrast is influenced by many factors, including scattering properties of the tissue [2], degree of polarization [11], illumination angle [10], and the ratio of pixel size to speckle size [6]. These factors are reflected in the beta term in [6]. This beta term and thus its effects on speckle contrast are expected to cancel out when calculating percentage change between the stimulation and basal conditions. Nonetheless, the blood-flow index T/τ_c estimated using the asymptotic approximation [Eq. (4)] are within 99.5% of that using the full equation (2c), consistent with Fig. 3. Moreover, the percent changes are essentially identical.

In summary, we demonstrated that the commonly used approximation in the LSI equation is valid when calculating blood-flow changes and introduced a time-efficient LSI analysis method. Moreover, we demonstrated a novel application of LSI by imaging blood flow of the rat retinas. Because blood flow is a critical physiological parameter and its perturbation has been implicated in the early stages of many retinal diseases, LSI has the potential to provide valuable physiologic information and to serve as an early surrogate marker for many retinal diseases.

This work is supported by the Department of Veterans Affairs (VISN7 VA Career Development Award) and the NIH (NEI R01-EY014211).

References

1. A. F. Fercher and J. D. Briers, *Opt. Commun.* **37**, 326 (1981).
2. U. Dirnagl, B. Kaplan, M. Jacewicz, and W. Pulsinelli, *J. Cereb. Blood Flow Metab.* **9**, 589 (1989).
3. A. K. Dunn, H. Bolay, M. A. Moskowitz, and D. A. Boas, *J. Cereb. Blood Flow Metab.* **21**, 195 (2001).
4. H. Bolay, U. Reuter, A. K. Dunn, Z. Huang, D. A. Boas, and M. A. Moskowitz, *Nat. Med.* **8**, 136 (2002).
5. H. Cheng, Q. Luo, Q. Liu, Q. Lu, H. Gong, and S. Zeng, *Phys. Med. Biol.* **49**, 1347 (2004).
6. R. Bandyopadhyay, A. S. Gittings, S. S. Suh, P. K. Dixon, and D. J. Durian, *Rev. Sci. Instrum.* **76**, 093110 (2005).
7. Z. Wang, S. Hughes, S. Dayasundara, and R. S. Menon, *Invest. Ophthalmol. Vis. Sci.* **27**, 258 (2007).
8. P. Zakharov, A. Volker, A. Buck, B. Weber, and F. Scheffold, *Opt. Lett.* **31**, 3465 (2006).
9. R. Bonner and R. Nossal, *Appl. Opt.* **20**, 2097 (1981).
10. J. W. Goodman, *Proc. IEEE* **53**, 1688 (1965).
11. J. W. Goodman, *Statistical Optics* (Wiley, 1985).
12. H. Cheng, Q. Luo, Z. Wang, H. Gong, S. Chen, W. Liang, S. Zeng, *Appl. Opt.* **42**, 5759 (2003).
13. A. C. Clermont, M. Brittis, T. Shiba, T. McGovern, G. L. King, and S. E. Bursell, *Invest. Ophthalmol. Visual Sci.* **35**, 981 (1994).
14. C. E. Riva, S. D. Cranstoun, R. M. Mann, and G. E. Barnes, *Invest. Ophthalmol. Visual Sci.* **35**, 608 (1994).

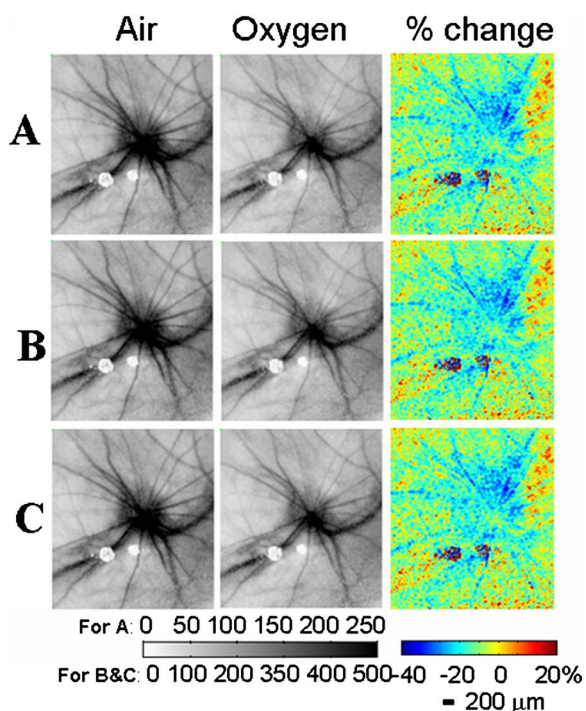


Fig. 3. (Color online) LSI blood-flow index and percent-change maps of a rat retina. LSI was performed while the animal was breathing air or oxygen. Percent-change maps are the differences between oxygen and air breathing. LSI maps were obtained using A, Newtonian iterative analysis of Method I without the factor $(1-\tau/T)$, Eq. (1b); B, Newtonian iterative analysis of Method II with the factor $(1-\tau/T)$, Eq. (2c); and C, simplified analysis of Method II with the factor $(1-\tau/T)$, Eq. (4). The LSI exposure time was 10 ms. Darker intensities correspond to higher blood flow. The two bright dots on the images are reflections off the corneal surface and/or lens.